

# A NOVEL LMI-BASED ROBUST MODEL PREDICTIVE CONTROL FOR DFIG-BASED WIND ENERGY CONVERSION SYSTEMS

AMIR GHOLAMI, ALIREZA SAHAB, ABDOLREZA TAVAKOLI AND BEHNAM ALIZADEH

The optimal and reliable performance of doubly fed induction generator is essential for the efficient and optimal operation of wind energy conversion systems. This paper considers the nonlinear dynamic of a DFIG linked to a power grid and presents a new robust model predictive control technique of active and reactive power by the use of the linear matrix inequality in DFIG-based WECS. The control law is obtained through the LMI-based model predictive control that allows considering both economic and tracking factors by optimization of an objective function, constraints on control signal and states of system and effects of nonlinearities, generator parameter uncertainties and external disturbances. Robust stability in the face of bounded disturbances and generator uncertainty is shown using Lyapunov technique. Numerical simulations show that the proposed control method is able to meet the desired specification in active and reactive power control in the presence of varieties of wind speed and pitch angle.

*Keywords:* linear matrix inequality, robust model predictive control, doubly fed induction generator, active and reactive power, optimization

*Classification:* 93C10, 93D09, 93C40, 93C42, 37N35

## 1. INTRODUCTION

In recent years, the ever-developing international interest in renewable energy resources is attracting massive consideration from both industry and academics due to the international increase in power demand, as well as the restriction of fossil fuels and their destructive impact on the environment. Of the many renewable generation resources, wind generation is considered as the most promising one and hence receiving international attentions [19]. Wind energy conversion systems (WECS) based on doubly fed induction generators (DFIGs) are the most used configuration nowadays, accounting for 50% of the wind energy generation market [14]. Doubly fed induction generators are widely used in modern wind turbines due to their full power control capability, variable speed operation, low converter cost, and reduced power loss compared to other solutions such as fixed speed induction generators or fully rated converter systems. From the view of the power system operation, it is desirable to regulate the active and reactive power of the DFIG under various wind conditions. Therefore, the control issues of the

DFIG are of great importance to be properly investigated. With many various purposes, the DFIG is controlled through many different control methods. For example, vector control is used based on either a stator voltage oriented [3, 11] or stator flux oriented vector [9, 10, 16] by using a d-q synchronous frame for separately controlling the active and reactive power through a current controller. In the mid-1980s, direct torque control (DTC) was studied in literature [4, 21, 26] to directly control the electromagnetic torque and the rotor flux of the DFIG by selecting the voltage vector from a predefined lookup table based on the stator flux and torque information. Based on the same fundamentals of the DTC technique, direct power control (DPC) was suggested to independently and directly control the active and reactive power of DFIG based on the estimated reactive and active power and their errors. For improving the power control, the authors in [12, 27] have proposed the scheme using the model-based predictive DPC technique.

Despite of the mentioned advanced control techniques, the changes of the dynamic parameters and external influences cause that DFIG is very difficult to control. Changing the dynamic parameters during operation will lead to a change in the output efficiency of the system. Another problem is the existence of a saturation phenomenon in controlling this system. Therefore, for the stability of the DFIG system, it is necessary to consider the combination of generator nonlinearity and the parameter uncertainty, the model dynamics, the velocity variability, and the saturation constraint on the control inputs in the controller design. So the designed controller should be able to consider changes to the system parameters and is designed in a way that it is not sensitive to parameter and structural variation of system model. In addition, the controller must be able to react against the wind changes and reduce disturbance and get the most efficiency of the DFIG system. Also, for optimal control, it is necessary to consider both the economic factors and the desired power track under realistic constraints. Accordingly, to increase DFIG-WCES's transient and steady state performance, in order to provide a satisfactory response to the output power with respect to the desired values, due to the errors caused by the disturbances of parameters and external disturbances, in this paper, a robust predictive control method is suggested as a tool for achieving the above objectives. The first attempt in robust MPC (RMPC) is the famous method of Min-Max MPC. In this method, the optimal control rule is designed for the worst uncertainty. This method was initially proposed as open loop control in [2], and its more complete solutions were presented in [15, 13]. In [13], a method for RMPC designed for systems with multidimensional and structural uncertainties is provided in the feedback loop. The problem of minimizing of upper bound on an infinite horizon, despite of constraints in the system at any sample time, is converted into a convex optimization problem in the linear matrix inequality (LMI) substrate. The most important features of the controller are: 1. simplicity of calculation and implementation; 2. the infinite prediction horizon that gives the best prediction of the future of the system. This method provides a systematic solution to the RMPC problem, which leads to a faster solution due to the use of LMI.

RMPC performs an optimization procedure to calculate optimal control actions at each sampling interval. It uses a model of the process explicitly to obtain the control signal by minimizing the objective function. So far, RMPC may be the advanced control strategy that can handle constraints, i.e., it can manipulate and control system vari-



## 2.1. Wind Turbine Model

The extracted mechanical power by means of wind turbine can be written as [7, 22]:

$$P_m = \frac{1}{2} \rho \pi R^2 C_p(\lambda, \beta) v_{wind}^2, \quad (1)$$

where  $\rho$  indicates the air density,  $R$  signifies the radius of the rotor of the turbine, and  $v_{wind}$  means the wind speed,  $C_p(\lambda, \beta)$  represents the power coefficient and it is a function of tip-speed-ratio  $\lambda$  and blade pitch angle  $\beta$ . A particular wind speed compares to a wind turbine rotational speed to get  $C_{Pmax}$ , namely, the maximum power coefficient, and so tracks the most extreme mechanical (wind) power. In common, the wind turbine works within the variable speed mode if wind speed does not exceed its rated value, then the rotational speed is adjusted by DFIG speed control so that  $C_p(\lambda, \beta)$  can be keep on at the  $C_{Pmax}$  point. However, in case wind turbine works over the rated wind speed, the pitch angle will be adjusted to ensure the operation safety of the wind turbine. At last, the tip-speed-ratio  $\lambda$  can be characterized as:

$$\lambda = \frac{\omega_m R}{v_{wind}}, \quad (2)$$

where  $\omega_m$  signifies the wind turbine rotational speed. According to the wind turbine characteristics, a generic equation of  $C_p(\lambda, \beta)$  can be defined by;

$$C_p(\lambda, \beta) = c_1 \left( \frac{c_2}{\lambda_i} - c_3 \beta - c_4 \right) e^{-\frac{c_5}{\lambda_i}} + c_6 \lambda \quad (3)$$

with:

$$\frac{1}{\lambda_i} = \frac{1}{\lambda + 0.08\beta} - \frac{0.035}{\beta^3 + 1}, \quad (4)$$

where  $c_1$  to  $c_6$  are fixed to:  $c_1 = 0.5176, c_2 = 116, c_3 = 0.4, c_5 = 21, c_6 = 0.0068$  respectively [7, 22].

## 2.2. Generator Model

The generator dynamics is presented by:

$$\begin{aligned} \frac{di_{qs}}{dt} &= \frac{\omega_b}{L'_s} \left( -R_1 i_{qs} + \omega_s L'_s i_{ds} + \frac{\omega_r}{\omega_s} e'_{qs} - \frac{1}{T_r \omega_s} e'_{ds} - v_{qs} + \frac{L_m}{L_{rr}} v_{qr} \right) \\ \frac{di_{ds}}{dt} &= \frac{\omega_b}{L'_s} \left( -R_1 i_{ds} - \omega_s L'_s i_{qs} + \frac{\omega_r}{\omega_s} e'_{ds} - \frac{1}{T_r \omega_s} e'_{qs} - v_{ds} + \frac{L_m}{L_{rr}} v_{dr} \right) \\ \frac{de'_{qs}}{dt} &= \omega_b \omega_s \left( R_2 i_{ds} + \left( 1 - \frac{\omega_r}{\omega_s} \right) e'_{ds} - \frac{1}{T_r \omega_s} e'_{qs} + \frac{L_m}{L_{rr}} v_{dr} \right) \\ \frac{de'_{ds}}{dt} &= \omega_b \omega_s \left( -R_2 i_{qs} - \left( 1 - \frac{\omega_r}{\omega_s} \right) e'_{qs} - \frac{1}{T_r \omega_s} e'_{ds} + \frac{L_m}{L_{rr}} v_{qr} \right), \end{aligned} \quad (5)$$

where  $\omega_b$  signifies the electrical base speed,  $\omega_s$  indicates the synchronous angle speed, and  $\omega_r$  means the rotor angle speed;  $e'_{ds}$  and  $e'_{qs}$  show the equal d-axis and q-axis ( $dq$ ) internal voltages;  $i_{ds}$  and  $i_{qs}$  state the dq-stator currents;  $v_{ds}$  and  $v_{qs}$  denote the dq-stator terminal voltages;  $v_{dr}$  and  $v_{qr}$  state the dq-rotor voltages.  $L_m$  implies the mutual

inductance; whereas the remaining parameters are given within the bellow.

$$\begin{aligned} \omega_b &= 100\pi \frac{\text{rad}}{\text{s}}, \omega_s = 1p.u, L_m = 4p.u, L_{ss} = 1.01L_m, L_{rr} = 1.005L_{ss}, H_m = 4.4s \\ R_s &= 0.005p.u, R_r = 1.1R_s, R = 58.59m^2, v_{wind} = 12 \frac{m}{s}, \beta = 15deg, \rho = 1.225 \frac{kg}{m^3} \\ L'_s &= L_{ss} - \frac{L_m^2}{L_{rr}}, R_2 = \left(\frac{L_m}{L_{rr}}\right)^2 R_r, T_r = \frac{L_{rr}}{R_r}, R_1 = R_s + R_2. \end{aligned} \quad (6)$$

The active power  $P_e$  supplied by the generator is considered by:

$$P_e = e'_{qs}i_{qs} + e'_{ds}i_{ds}. \quad (7)$$

The q-axis is adjusted with the stator voltage whereas the d-axis is adjusted to lead the q-axis, in this way,  $v_{ds} \equiv 0$  and  $v_{qs}$  matches to the terminal voltage magnitude. The reactive power  $Q_e$  is achieved as:

$$Q_e = v_{qs}i_{ds} + v_{ds}i_{qs}. \quad (8)$$

### 2.3. Shaft System Model

The shaft framework can be modelled as a single lumped-mass system, whose lumped inertia constant  $H_\infty$  is considered as [18]:

$$H_m = H_t + H_g, \quad (9)$$

where  $H_t$  and  $H_g$  specify the inertia constants of wind turbine and generator, respectively. The electromechanical dynamics is defined as:

$$\frac{d\omega_m}{dt} = \frac{1}{2H_m} (T_m - T_e - D\omega_m), \quad (10)$$

where  $\omega_m$  is the rotational speed of the lumped-mass system and is equal to the generator rotor speed  $\omega_r$  when both of them given in per unit;  $D$  signifies the lumped system damping; and  $T_m$  is the mechanical torque with  $T_m = \frac{P_m}{\omega_m}$ , respectively.

## 3. RMPC DESIGN OF DFIG FOR POWER SYSTEM STABILITY ENHANCEMENT

Consider the following continuous-time nonlinear systems

$$\dot{x}(t) = Ax(t) + Bu(t) + w(t, x), \quad (11)$$

where  $x(t) \in R^{n_x}$  shows the system states,  $u(t) \in R^{n_u}$  is the control input, The signal  $w(t) \in R^{n_w}$  is the disturbance or model-plant mismatch, which is unknown but bounded, and lies in a compact set,

$$W = \{w(t) \in R^{n_w} \mid \|w\| \leq w_{max}\}. \quad (12)$$

The system has the following boundaries  $x(t) \in X$ ,  $u(t) \in U$ ,  $\forall t > 0$ . Where,  $X \subset R^{n_x}$  is bounded and  $U \subset R^{n_u}$  is compact.

**Lemma 3.1.** (Yu et al. [25]) Let  $S : R^{n_x} \rightarrow [0, \infty)$  be a continuously differentiable function and  $\alpha_1(\|x\|) < S(x) < \alpha_2(\|x\|)$ , where  $\alpha_1, \alpha_2$  are class  $k_\infty$  functions. Suppose  $u : R \rightarrow R^{n_u}$  is chosen, and there exist  $\lambda > 0$  and  $\mu > 0$  such that

$$\dot{S}(x) + \lambda S(x) - \mu w^T(t) w(t) \leq 0 \tag{13}$$

with  $x \in X, d \in D$ . Then, the system trajectory starting from  $x(t_0) \in \Omega \subseteq X$ , will remain in the set  $\Omega$ , where

$$\Omega = \left\{ x \in R^{n_x} \mid S(x) \leq \frac{\mu w_{\max}^2}{\lambda} \right\}. \tag{14}$$

**Lemma 3.2.** (Poursafar et al. [17]) Let  $M, N$  be real constant matrices and  $P$  be a positive matrix of compatible dimensions. Then

$$M^T P N + N^T P M \leq \varepsilon M^T P M + \varepsilon^{-1} N^T P N \tag{15}$$

holds for any  $\varepsilon > 0$ .

**Lemma 3.3.** (Bpyd et al. [1]) The LMI

$$\begin{bmatrix} Q(x) & S(x) \\ S^T(x) & R(x) \end{bmatrix} > 0. \tag{16}$$

In which,  $Q(x) = Q^T(x), R(x) = R^T(x)$  and  $S(x)$  are affine function of  $x$ , and is corresponding to

$$\begin{aligned} R(x) > 0 \quad & Q(x) - S(x)R^{-1}(x)S^T(x) > 0 \\ Q(x) > 0 \quad & R(x) - S(x)Q^{-1}(x)S^T(x) > 0. \end{aligned} \tag{17}$$

By choosing the tracking error  $e = [ e_1 \quad e_2 ]^T$  for active power  $P_e$  and reactive power  $Q_e$  as the outputs, it yields

$$\begin{aligned} e_1 &= P_e - P_e^* \\ e_2 &= Q_e - Q_e^*, \end{aligned} \tag{18}$$

where  $P_e^*$  and  $Q_e^*$  signify the active and reactive power references, respectively. The differentiate tracking error (18) for explicitly appearing the control inputs  $v_{qr}$  and  $v_{dr}$ , gives

$$\begin{bmatrix} \dot{e}_1 \\ \dot{e}_2 \end{bmatrix} = \begin{bmatrix} -\frac{R_1 \omega_b}{L'_s} - \frac{\omega_b}{T_r} & 0 \\ 0 & -\frac{R_1 \omega_b}{L'_s} \end{bmatrix} \begin{bmatrix} e_1 \\ e_2 \end{bmatrix} + \begin{bmatrix} f_1 \\ f_2 \end{bmatrix} + \begin{bmatrix} B_{11} & B_{12} \\ B_{21} & B_{22} \end{bmatrix} \begin{bmatrix} v_{qr} \\ v_{dr} \end{bmatrix}, \tag{19}$$

where

$$\begin{aligned}
 f_1 &= -\frac{\omega_b}{L'_s} v_{qs} e'_{qs} - \frac{\omega_b}{L'_s} v_{ds} e'_{ds} + \frac{\omega_b \omega_r}{L'_s \omega_s} (e'^2_{qs} + e'^2_{ds}) + \omega_b \omega_r (e'_{qs} i_{ds} - e'_{ds} i_{qs}) \\
 &\quad - \left( \frac{R_1 \omega_b}{L'_s} + \frac{\omega_b}{T_r} \right) P_e^* - \dot{P}_e^* \\
 f_2 &= -\omega_b \omega_s (v_{qs} i_{qs} + v_{ds} i_{ds}) + \frac{\omega_b}{L'_s T_r \omega_s} (v_{qs} e'_{qs} + v_{ds} e'_{ds}) + \frac{\omega_b \omega_r}{L'_s \omega_s} (v_{qs} e'_{ds} - v_{ds} e'_{qs}) \\
 &\quad - \frac{R_1 \omega_b}{L'_s} Q_e^* - \dot{Q}_e^* \\
 B_{11} &= \frac{L_m \omega_b}{L_{rr} L'_s} e'_{qs} + \frac{L_m \omega_b \omega_s}{L_{rr}} i_{ds} \\
 B_{12} &= \frac{L_m \omega_b}{L_{rr} L'_s} e'_{ds} - \frac{L_m \omega_b \omega_s}{L_{rr}} i_{qs} \\
 B_{21} &= -\frac{L_m \omega_b}{L_{rr} L'_s} v_{ds} \\
 B_{22} &= \frac{L_m \omega_b}{L_{rr} L'_s} v_{qs},
 \end{aligned} \tag{20}$$

where  $f_1$  and  $f_2$  contain the combinatorial impact of nonlinearities, generator parameter uncertainties, and external disturbances. Moreover,  $B$  is the original control gain matrix which elements also cover uncertain generator parameters.

Assume all nonlinearities and parameters are unknown, state the perturbations  $\psi_1(\cdot)$  and  $\psi_2(\cdot)$  for system (19) to combined all the nonlinearities, generator uncertainties, and external disturbances of  $f_1$ ,  $f_2$  and  $B$  into a lumped term, such that they can be rewritten into a brief form, it gives

$$\begin{bmatrix} \psi_1(\cdot) \\ \psi_2(\cdot) \end{bmatrix} = \begin{bmatrix} f_1 \\ f_2 \end{bmatrix} + (B - B_0) \begin{bmatrix} v_{qr} \\ v_{dr} \end{bmatrix}, \tag{21}$$

where  $B_0$  is the new control gain as following

$$B_0 = \begin{bmatrix} b_{11} & 0 \\ 0 & b_{22} \end{bmatrix}. \tag{22}$$

In the above equation,  $b_{11}$  and  $b_{22}$  are constants. Here, the new control gain  $B_0$  is chosen in such way to completely decouple the control of active power and reactive power.

Then system (19) can be adjusted as

$$\begin{bmatrix} \dot{e}_1 \\ \dot{e}_2 \end{bmatrix} = \begin{bmatrix} -\frac{R_1 \omega_b}{L'_s} - \frac{\omega_b}{T_r} & 0 \\ 0 & -\frac{R_1 \omega_b}{L'_s} \end{bmatrix} \begin{bmatrix} e_1 \\ e_2 \end{bmatrix} + \begin{bmatrix} \psi_1(\cdot) \\ \psi_2(\cdot) \end{bmatrix} + \begin{bmatrix} b_{11} & 0 \\ 0 & b_{22} \end{bmatrix} \begin{bmatrix} v_{qr} \\ v_{dr} \end{bmatrix}. \tag{23}$$

Here, the above two first order differential equations define the decoupled dynamics of active power and reactive power, respectively.

By definition

$$\begin{aligned}
 v_{qr} &= u_1 + v_1 \\
 v_{dr} &= u_2 + v_2,
 \end{aligned} \tag{24}$$

where  $v_1$  and  $v_2$  are relevant to the state feedback and  $u_1$  and  $u_2$  are related to the robust predictive control.

System states arrive at the point of equilibrium under the state feedback and the robust predictive control unit ensures system stability against uncertainties. To get the state feedback rule, we consider the subsystem (25).

$$\begin{bmatrix} \dot{e}_1 \\ \dot{e}_2 \end{bmatrix} = \begin{bmatrix} -\frac{R_1\omega_b}{L'_s} - \frac{\omega_b}{T_r} & 0 \\ 0 & -\frac{R_1\omega_b}{L'_s} \end{bmatrix} \begin{bmatrix} e_1 \\ e_2 \end{bmatrix} + \begin{bmatrix} b_{11} & 0 \\ 0 & b_{22} \end{bmatrix} \begin{bmatrix} v_{qr} \\ v_{dr} \end{bmatrix}. \tag{25}$$

By choosing Lyapunov function in the following way:

$$V(e_1, e_2) = \frac{1}{2}e_1^2 + \frac{1}{2}e_2^2, \tag{26}$$

which is a positive definite function. In order to guarantee the stability, the derivative of the Lyapunov function must be determined negatively. For this purpose

$$\dot{V}(e_1, e_2) = e_1 \left( -\left( \frac{R_1\omega_b}{L'_s} + \frac{\omega_b}{T_r} \right) e_1 + b_{11}v_1 \right) + e_2 \left( -\frac{R_1\omega_b}{L'_s} e_2 + b_{22}v_2 \right). \tag{27}$$

By selecting

$$\begin{aligned} v_1 &= -k_1 e_1 \\ v_2 &= -k_2 e_2 \end{aligned} \tag{28}$$

we will have

$$\dot{V}(e_1, e_2) = -\left( \frac{R_1\omega_b}{L'_s} + \frac{\omega_b}{T_r} + b_{11}k_1 \right) e_1^2 - \left( \frac{R_1\omega_b}{L'_s} + b_{22}k_2 \right) e_2^2. \tag{29}$$

Applying (28) to (23) and rewriting it, we will have

$$\begin{aligned} \begin{bmatrix} \dot{e}_1 \\ \dot{e}_2 \end{bmatrix} &= \begin{bmatrix} -\left( \frac{R_1\omega_b}{L'_s} + \frac{\omega_b}{T_r} + b_{11}k_1 \right) & 0 \\ 0 & -\left( \frac{R_1\omega_b}{L'_s} + b_{22}k_2 \right) \end{bmatrix} \\ \begin{bmatrix} e_1 \\ e_2 \end{bmatrix} &+ \begin{bmatrix} \psi_1(\cdot) \\ \psi_2(\cdot) \end{bmatrix} + \begin{bmatrix} b_{11} & 0 \\ 0 & b_{22} \end{bmatrix} \begin{bmatrix} u_1 \\ u_2 \end{bmatrix}. \end{aligned} \tag{30}$$

Now, to control the system (30), we will apply a robust model predictive control. For system (30), the state-feedback control law in  $kT$  time is selected as

$$u(kT + \tau, kT) = Ke(kT + \tau, kT). \tag{31}$$

The infinite horizon quadratic cost function is stated as

$$\begin{aligned} J &= \int_0^\infty (e(kT + \tau, kT)^T Q e(kT + \tau, kT) \\ &\quad + u(kT + \tau, kT)^T R u(kT + \tau, kT) \\ &\quad + \mu w(kT + \tau, kT)^T w(kT + \tau, kT)) d\tau, \quad \mu > 0, \end{aligned} \tag{32}$$

where  $Q$  and  $R$  are positive definite weight matrices. In the objective function (32), the uncertain but negative effect with weight  $\mu$  is presented, where  $\mu$  is acquired by  $H_\infty$  technique [20].

**Theorem 3.4.** Consider system (30) where  $e(kT)$  is the measure value in sampling time of  $kT$ . There is a state-feedback control law (31) in true stability condition, if the optimization problem with LMI constraints can be feasible.

$$\begin{aligned} & \min_{\gamma, X} \gamma \\ & \begin{bmatrix} I & e(kT)^T \\ e(kT) & X \end{bmatrix} \\ & (AX + BY)^T + AX + BY + (\alpha + \lambda)X \leq 0 \\ & -X + \gamma \varepsilon^{-1} I \leq 0, \end{aligned} \tag{33}$$

where  $X > 0$  and  $Y$  are matrixes achieved from the aforementioned optimization problem and  $\gamma$  is a positive scalar (the upper bound of the objective (32)). As such, state-feedback matrix is achieved as  $K = YX^{-1}$  in every moment.

*Proof.* Consider the following quadratic Lyapunov function

$$V(e(t)) = e(t)^T P e(t), P > 0. \tag{34}$$

In sampling time for  $kT$  assume that  $V(e(t))$  holds true in the following condition

$$e(t)^T P e(t) < \gamma \tag{35}$$

$$\begin{aligned} \frac{dV(e(kT+\tau, kT))}{dt} & \leq -(e(kT + \tau, kT)^T Q e(kT + \tau, kT) \\ & u(kT + \tau, kT)^T R u(kT + \tau, kT) \\ & \mu w(kT + \tau, kT)^T w(kT + \tau, kT)). \end{aligned} \tag{36}$$

With the purpose of obtaining the robust efficiency, it must be  $e(\infty, kT) = 0$  which results in  $V(e(\infty, kT)) = 0$ . With the integration of the both sides of the equation (36) is obtained

$$J \leq V(e(kT)). \tag{37}$$

With the intention of obtaining an MPC robust algorithm, the Lyapunov function should be minimized taking into consideration the upper bound [8]. Thus

$$\begin{aligned} & \min_{\gamma, P} \gamma \quad \text{subject to} \\ & e(t)^T P e(t) \leq \gamma. \end{aligned} \tag{38}$$

By describing  $X = \gamma P^{-1}$  and utilizing Schur Complements, we have

$$\begin{aligned} & \min_{\gamma, X} \gamma \\ & \begin{bmatrix} I & x(kT)^T \\ x(kT) & X \end{bmatrix} \geq 0. \end{aligned} \tag{39}$$

In continue, as stated by Lemma 3.1, for system (30) we have

$$\dot{S}(e(t)) + \lambda S(e(t)) - \mu w(t, e)^T w(t, e) \leq 0. \tag{40}$$

Then, in accordance with (34), it can be achieved

$$\dot{e}(t)^T P e(t) + e(t)^T P \dot{e} + \lambda e(t)^T P e(t) - \mu w(t, e)^T w(t, e) \leq 0 \tag{41}$$

$$e(t)^T ((A + BK)^T P + P(A + BK) + \lambda P) e(t) + w(t, e)^T P e(t) + e(t)^T P w(t, e) - \mu w(t, e)^T w(t, e) \leq 0 \tag{42}$$

with respect to Lemma 3.2

$$w(t, e)^T P e(t) + e(t)^T P w(t, e) \leq \alpha e(t)^T P e(t) + \alpha^{-1} w(t, e)^T P w(t, e) \tag{43}$$

By replacing (43) in (42), it is gotten that

$$e(t)^T ((A + BK)^T P + P(A + BK) + (\alpha + \lambda)P) e(t) + \alpha^{-1} w(t, e)^T P w(t, e) - \mu w(t, e)^T w(t, e) \leq 0. \tag{44}$$

By considering

$$P \leq \lambda_{\max} I \leq \varepsilon I, \tag{45}$$

where  $\lambda_{\max}$  indicates the maximum eigenvalue of  $P$  and  $\varepsilon I$  specifies the corresponding upper bound [17], then

$$e(t)^T ((A + BK)^T P + P(A + BK) + (\alpha + \lambda)P) e(t) + (\alpha^{-1} \varepsilon - \mu) w(t, e)^T w(t, e) \leq 0. \tag{46}$$

By selecting

$$\mu = \frac{\varepsilon}{\alpha}. \tag{47}$$

Equation (46) is concentrated to

$$e(t)^T ((A + BK)^T P + P(A + BK) + (\alpha + \lambda)P) e(t) \leq 0. \tag{48}$$

Replacing  $P = \gamma X^{-1}$ ,  $X > 0$  and  $K = Y X^{-1}$ ,

$$((A + B Y X^{-1})^T X^{-1} + X^{-1}(A + B Y X^{-1}) + (\alpha + \lambda)X^{-1}) \gamma \leq 0. \tag{49}$$

By pre and post multiplying  $X$ ,

$$(A X + B Y)^T + A X + B Y + (\alpha + \lambda)X \leq 0. \tag{50}$$

According to (45), it is obvious

$$P \leq \varepsilon I. \tag{51}$$

Replacing  $P = \gamma X^{-1}$  and by pre multiplying  $X$ , it can be obtained

$$-X + \gamma \varepsilon^{-1} I \leq 0. \tag{52}$$

So, the proof is completed. □

#### 4. SIMULATION

In this section, the robust model predictive control is applied to the DFIG system. Also, to prove the dominance of the proposed controller, it is compared with RPC [5].

##### 4.1. Step change of wind speed

At fixed pitch angle of 15 deg, the wind speed is changed from 10 to 12 m/s (10 m/s<sup>2</sup> rate) and it affects the output power of the wind turbine according to the equations 1-4. Figure 2 shows the wind speed profile and system responses and control costs. It is obvious that the active power oscillation continues for a 5 s in RPC control whereas RMPC can successfully suppress such unfavorable oscillation in less than 0.5 s, plus the minimal overshoot among two methods. Additionally, RMPC desires the least control efforts compared to that of RPC control. Even though RMPC reconstruct the reactive power slower than that of RPC control, it provides a much smoother response with less overshoot.

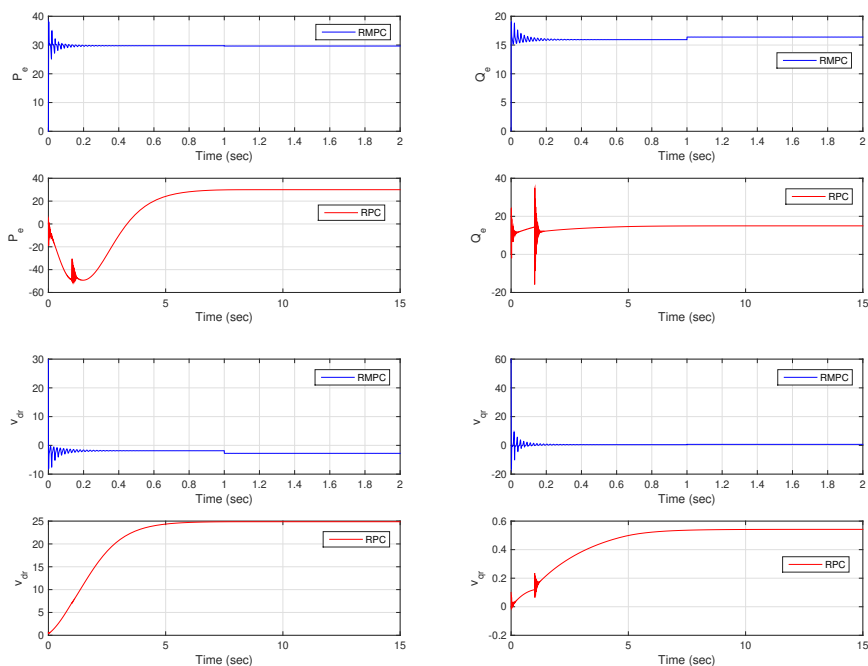


**Fig. 2.** System responses and control costs obtained under a step change of wind speed from 10 to 12 m/s with a fixed pitch angle of 15 deg. (a) active power; (b) reactive power; (c) d-axis rotor voltage; (d) q-axis rotor voltage.

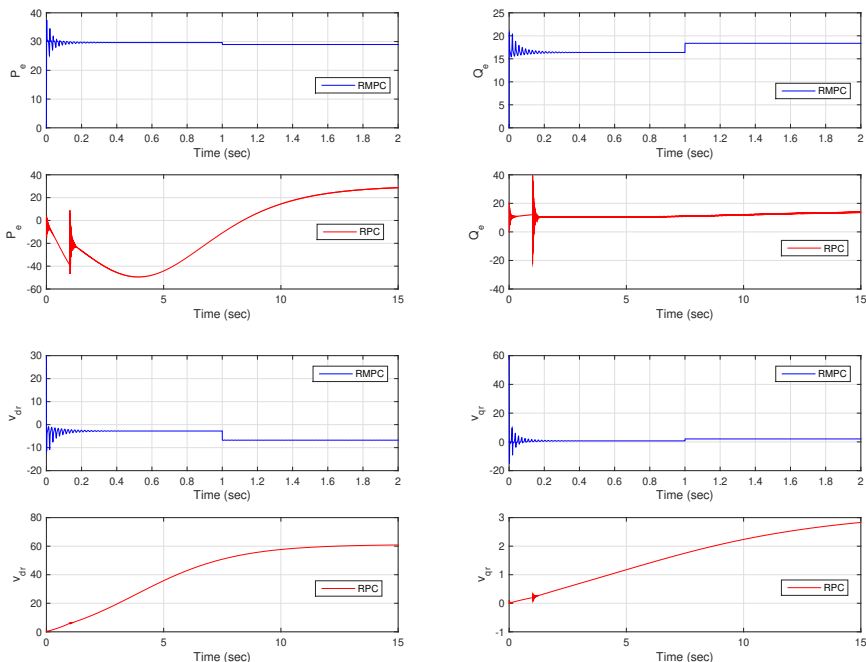


**Fig. 3.** System responses obtained under a pitch angle variation from 15 to 5 deg. in 1 s with a constant wind speed of 12 m/s. (a) active power; (b) reactive power.;(c) d-axis rotor voltage; (d) q-axis rotor voltage.

### 4.2. Pitch angle variation

While pitch angle is very critical for the wind power production and safe process of wind turbine [6], the control performance of RMPC is compared against to that of RPC. At constant wind speed of 12 m/s, the pitch angle decreases from 15 to 5 deg. in 1 s. Figure 3 shows the system responses, which demonstrates that the active power of RMPC can meet around 0.5 s, whereas RPC control have to be expend 10 s. Additionally, RMPC needs the slightest control costs compared to that of RPC control.

The comparisons show that the RMPC strategy based on the nonlinear DFIG model can effectively track the given power set points in the presence of wind speed and pitch angle variations regardless of optimizing the cost function and considering constraints.

### 4.3. Low frequency disturbance

In this section, low frequency inter-area modes oscillation is considered as external disturbance. This kind of oscillation is common among multiple groups of generators [24] and should be suppressed. For this purpose,  $v_s = 1 + 0.1 \sin(\pi t/1.25)$  is applied to the system as an inter-area type disturbance. The responses obtained from the simulation

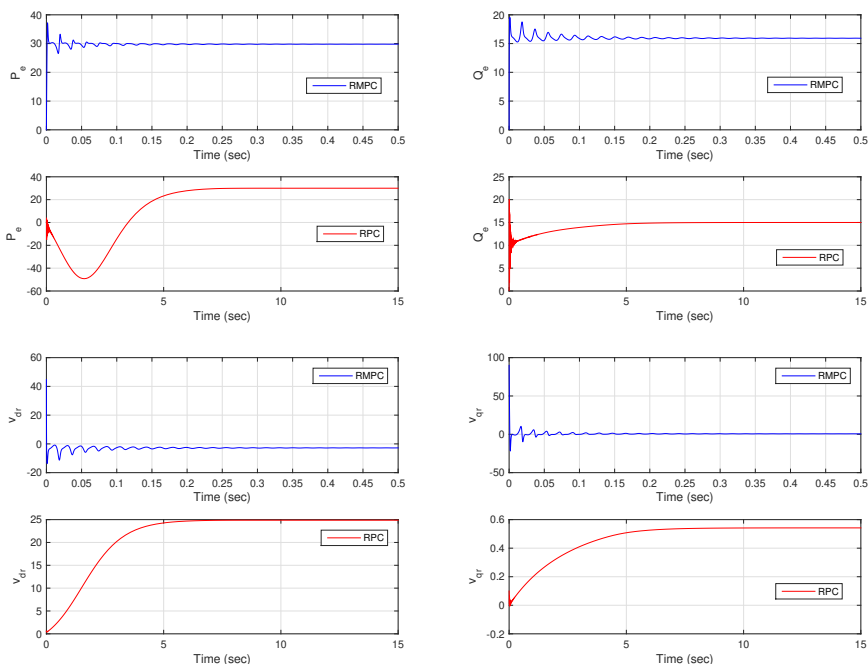


**Fig. 4.** The responses obtained under low frequency disturbance  $v_s = 1 + 0.1 \sin(\pi t/1.25)$ . (a) active power; (b) reactive power speed.

are shown in Figure 4. As it can be seen from the figure, the RMPC in a much shorter time and with less fluctuations than RPC is able to eliminate the effects of disturbance on the system and achieve the target  $P$  and  $Q$  values.

#### 4.4. Model uncertainty

To evaluate the robustness of the proposed method under model uncertainty, the following scenario is considered: The  $L_m$  changes around its nominal value of  $\pm 20\%$ , and this change also affects other parameters of the model. The active and reactive power obtained from the simulation are shown in Figure 5. The results are roughly similar to the results of Section 4.3, namely, by using RMPC, the elimination of uncertainty effects is obtained in a shorter time with less fluctuation.

The above simulations demonstrate the capability of the proposed method in optimal and robust control of the DFIG system. The simulation is executed on Matlab (2014b MathWorks) using a personal computer with an Intel(R) Core(TM) i7 CPU at 2.2 GHz and 8 GB of RAM and execution times of 0.76644s, 0.72121s, 0.57842s and 0.63716s were obtained for scenarios 4.1 to 4.4, respectively.

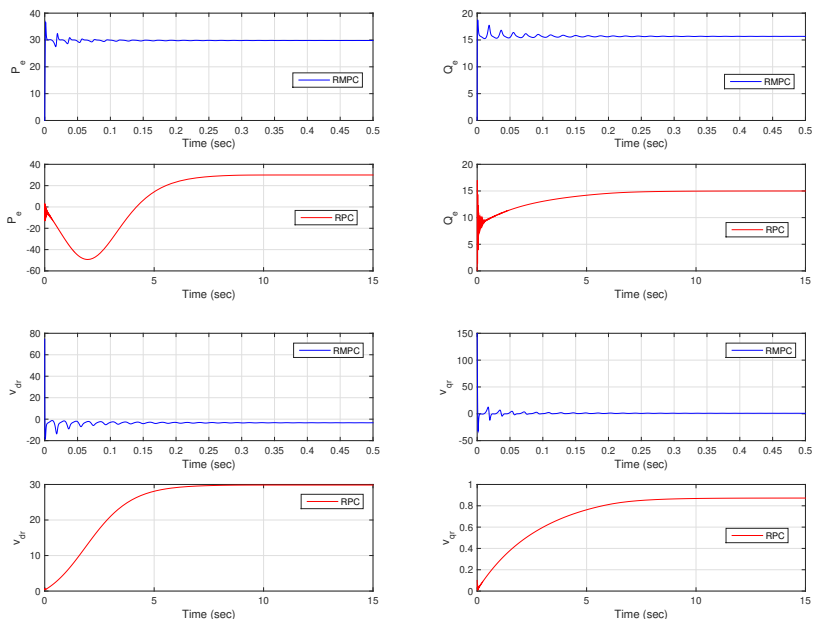


**Fig. 5.** System responses obtained under  $L_m$  uncertainty. (a) active power; (b) reactive power

### 5. CONCLUSION

An LMI-based RMPC strategy for DFIG-based WECS has been proposed in this paper. A nonlinear DFIG model was considered and the predicted active and reactive output power were calculated using a state space model resulting the nonlinear DFIG model. The control law is derived from LMI based RMPC that considers control tracking and economic index through optimization of an objective function, while considering the constraints on the states and the control signal. It is shown that the performance of the proposed RMPC is superior to that of RPC method. Therefore, the proposed RMPC provides a useful method for controlling this class of nonlinear DFIG in the operation of WECS in presence of wind variation and parameter uncertainty.

### ACKNOWLEDGEMENT

The authors would like to thank referees for their constructive comments.

(Received November 17, 2018)

## REFERENCES

- 
- [1] S. Boyd, L. Ghai, E. Feron, and V. Balakrishnan: Linear Matrix Inequalities in Control Theory. SIAM, Philadelphia 1994. DOI:10.1137/1.9781611970777
  - [2] P. Campo and M. Morari: Robust model predictive control. In: Proc. American Control Conference, Minneapolis 1987.
  - [3] S. Chondrogiannis and M. Barnes: Stability of doubly-fed induction generator under stator voltage orientated vector control. *IET Renew. Power Gener.* *2* (2008), 170–180. DOI:10.1049/iet-rpg:20070086
  - [4] M. Depenbrock: Direct self-control (DSC) of inverter-fed induction machine. *IEEE Trans. Power Electron.* *3* (1988), 420–429. DOI:10.1109/63.17963
  - [5] J. Dong, S. Li, S. Wu, T. He, B. Yang, H. Shu, and J. Yu: Nonlinear observer-based robust passive control of doubly-fed induction generators for power system stability enhancement via energy reshaping. *Energies* *10* (2017), 8, 1082. DOI:10.3390/en10081082
  - [6] M. Duong, F. Grimaccia, S. Leva, M. Mussetta, and E. Ogliari: Pitch angle control using hybrid controller for all operating regions of SCIG wind turbine system. *Renew. Energy* *70* (2014), 197–203. DOI:10.1016/j.renene.2014.03.072
  - [7] M. Fei and B. Pal: Modal analysis of grid-connected doubly fed induction generators. *IEEE Trans. Energy Convers* *22* (2007), 728–736. DOI:10.1109/tec.2006.881080
  - [8] V. Ghaffari, S. Vahid Naghavi, A. A. Safavi, and M. Shafiee: An LMI framework to design robust MPC for a class of nonlinear uncertain systems. In: Control Conference (ASCC), Asian 2013. DOI:10.1109/ascc.2013.6606169
  - [9] S. Hao, E. Abdi, F. Barati, and R. McMahon: Stator-flux-oriented vector control for brushless doubly fed induction generator. *IEEE Trans. Ind. Electron.* *56* (2009), 4220–4228. DOI:10.1109/tie.2009.2024660
  - [10] B. Hopfensperger, D. Atkinson, and R. Lakin: Stator-flux-oriented control of a doubly-fed induction machine with and without position encoder. *IEE Proc. Electr. Power Appl.* *147* (2000), 241–250. DOI:10.1049/ip-epa:20000442
  - [11] J. Hu, Y. He, L. Xu, and B. Williams: Improved control of DFIG systems during network unbalance using PI-R current regulators. *IEEE Trans. Ind. Electron.* *56* (2009), 439–451. DOI:10.1109/tie.2008.2006952
  - [12] J. Hu, J. Zhu, and D. Dorrell: Model-predictive direct power control of doubly-fed induction generators under unbalanced grid voltage conditions in wind energy applications. *IET Renew. Power Gener.* *8* (2014), 687–695. DOI:10.1049/iet-rpg.2013.0312
  - [13] M. Kothare, V. Balakrishnan, and M. Morari: Robust constrained model predictive control using linear matrix inequalities. *Automatica* *32* (1996), 10, 1361–1379. DOI:10.1016/0005-1098(96)00063-5
  - [14] M. Liserre, R. Cardenas, M. Molinas, and J. Rodriguez: Overview of multi-MW wind turbines and wind parks. *IEEE Trans. Ind. Electron.* *58* (2011), 4, 1081–1095. DOI:10.1109/tie.2010.2103910
  - [15] Y. Lu and Y. Arkun: Quasi-min-max MPC algorithms for LPV systems. *Automatica* *36* (2000), 4, 527–540. DOI:10.1016/s0005-1098(99)00176-4
  - [16] R. Pena, J. Clare, and G. Asher: Doubly fed induction generator using back-to-back PWM converters and its application to variable-speed wind-energy generation. *IEE Proc. Electr. Power Appl.* *143* (1996), 231–241. DOI:10.1049/ip-epa:19960288

- [17] N. Poursafar, H. Taghirad, and M. Haeri: Model predictive control of nonlinear discrete time systems: a linear matrix inequality approach. *IET Proc. Control Theory Appl.* *4* (2010), 1922–1932. DOI:10.1049/iet-cta.2009.0650
- [18] W. Qiao: Dynamic modeling and control of doubly fed induction generators driven by wind turbines. In: *Proc. IEEE/PES Power Systems Conference and Exposition, Seattle 2009*. DOI:10.1109/psce.2009.4840245
- [19] X. Sun, B. Zhang, X. Tang, B. McLellan, and M. Höök: Sustainable energy transitions in China: Renewable. *Energies* *9* (2016), 980. DOI:10.3390/en9120980
- [20] F. Tahir and I.M. Jaimoukha: Robust model predictive control through dynamic state-feedback: An LMI approach. *IFAC Proc. Vol. 40* (2011), 1, 3672–3677. DOI:10.3182/20110828-6-it-1002.03112
- [21] I. Takahashi and T. Noguchi: A new quick-response and high-efficiency control strategy of an induction motor. *IEEE Trans. Ind. Appl.* (1986), 820–827. DOI:10.1109/tia.1986.4504799
- [22] B. Yang, L. Jiang, L. Wang, W. Yao, and Q. Wu: Nonlinear maximum power point tracking control and modal analysis of DFIG based wind turbine. *Int. J. Electr. Power Energy Syst.* *74* (2016), 429–436. DOI:10.1016/j.ijepes.2015.07.036
- [23] B. Yang, X. Zhang, T. Yu, H. Shu, and Z. Fang: Grouped grey wolf optimizer for maximum power point tracking of doubly-fed induction generator based wind turbine. *Energy Convers. Manag.* *133* (2017), 427–443. DOI:10.1016/j.enconman.2016.10.062
- [24] W. Yao, J. Lin, W. Jinyu, W. Qinghua, and C. Shijie: Wide-area damping controller for power system inter-area oscillations: A networked predictive control approach. *IEEE Trans. Control Syst. Technol.* *23* (2015), 27–37. DOI:10.1109/tcst.2014.2311852
- [25] S.-Y. Yu, C. Bohm, H. Chen, and F. Allgower: Robust model predictive control with disturbance invariant sets. In: *Proc. Amer. Contr. Conf., Baltimore 2010*. DOI:10.1109/acc.2010.5531520
- [26] D. Zhi and L. Xu: Direct power control of DFIG with constant switching frequency and improved transient performance. *IEEE Trans. Energy Convers.* *22* (2007), 110–118. DOI:10.1109/tec.2006.889549
- [27] D. Zhi, L. Xu, and B. Williams: Model-based predictive direct power control of doubly fed induction generators. *IEEE Trans. Power Electron.* *25* (2010), 341–351. DOI:10.1109/tpel.2009.2028139

*Amir Gholami, PhD. candidate. Lahijan Branch, Department of Electrical Engineering, Islamic Azad University. Iran.*

*Alireza Sahab, Assistant Professor, Corresponding author. Lahijan Branch, Department of Electrical Engineering, Islamic Azad University. Iran.*

*e-mail: sahab@liau.ac.ir*

*Abdolreza Tavakoli, Assistant Professor. Lahijan Branch, Department of Electrical Engineering, Islamic Azad University. Iran.*

*Behnam Alizadeh, Assistant Professor. Lahijan Branch, Department of Electrical Engineering, Islamic Azad University. Iran.*